Int. J. Solids Structures Vol. 19, No. 5, pp. 411–424, 1983
Printed in Great Britain.

0020-7683/83/050411-14$03.00/0
Pergamon Press Ltd.

VIBRATIONS OF CANTILEVERED DOUBLY-CURVED SHALLOW SHELLS

A. W. LEISSA, J. K. LEE and A. J. WANG
Department of Engineering Mechanics, Ohio State University, Columbus, OH 43210, U.S.A.

(*Received* 22 *March* 1982)

Abstract—Vibrational characteristics are determined for a previously unsolved class of problems, that of doubly-curved shallow shells having rectangular planforms, clamped along one edge and free on the other three. The solution procedure uses the Ritz method with algebraic polynomial trial functions. Convergence studies are made, and accurate frequencies and contour plots of mode shapes are presented for various curvature ratios, including spherical, circular cylindrical and hyperbolic paraboloidal shells. Particular emphasis is given to the effect of adding spanwise curvature to shells having chordwise curvature; numerous published references already exist for the case of zero spanwise curvature. The effects of changing aspect ratio, thickness ratio and Poisson's ratio are also studied.

1. INTRODUCTION

The literature of shell vibrations is vast. A monograph summarizing the literature through the year 1971 listed approx. 1000 references[1]. Since that time many more have appeared. But approx. 95% of this literature deals with closed shells having various curvatures (e.g. circular cylindrical, noncircular cylindrical, conical, spherical, ellipsoidal), while open shells have received little attention.

Some researchers have investigated shells with shallow, circular cylindrical curvature, having a rectangular planform defined by two edges along generators and the other two along meridians. Special attention has been given[2–5] to the case when one meridian is clamped and the other three edges are free (Fig. 1b). This configuration represents a first approximation to an untwisted turbomachinery blade. A recent survey article[6] listed 23 references dealing with this problem, most of them being finite element analyses utilizing various types of elements.

However, it appears that the vibrations of cantilevered shells having both chordwise and spanwise (i.e. in directions parallel and perpendicular to the clamped boundary) curvature (Fig. 2) have not been previously considered. Such shells also have practical application; indeed, some advanced designs of turbomachinery blades have significant curvature in both directions. This leads one to wonder: "What is the effect of additional spanwise curvature upon the vibration frequencies and mode shapes of cantilevered shells having chordwise curvature and rectangular planform?" In particular, does the addition of spanwise curvature cause the frequencies to increase or decrease? Does the result depend upon whether the resulting Gaussian curvature ($1/R_xR_y$) is positive (Fig. 1a) or negative (Fig. 1c)? Does the result depend upon the vibration mode being considered? The primary purpose of this paper is to present an analytical procedure for solving such problems and to answer the aforementioned questions.

These questions have been answered for the case of the shallow shell of rectangular planform supported on all edges by shear diaphragms (also called "freely supported" or "simply supported" elsewhere in the literature). For this case an exact, closed form solution exists for the eigenvalues (frequencies) and eigenfunctions (mode shapes) of free vibration, and numerical results are easily calculated. It was shown[7] that increasing positive Gaussian curvature causes the frequencies of all modes to be increased, whereas negatively changing values of R_y/R_x cause first decreasing, then increasing frequencies. For example, the fundamental frequencies of relatively thin ($R_x/h = 1000$), shallow ($b/R_y = 0.4$) shells having square planform ($a/b = 1$) and representative material ($\nu = 0.3$) were found to be in the approximate ratio 1:13:26 for shells of hyperbolic paraboloidal, circular cylindrical and spherical curvature (i.e. $R_y/R_x = -1$, 0 and 1), respectively.

For the present problem no exact solution is possible. However, the Ritz method is employed in such a manner as to obtain frequencies as close to the exact values as desired. The classical shallow shell theory (see [8–10]) is used, and the three components of displacement are

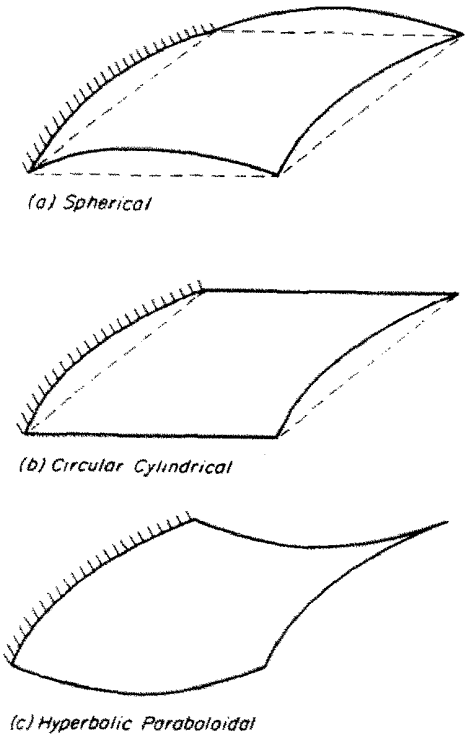

Fig. 1. Shells of positive, zero and negative Gaussian curvature.

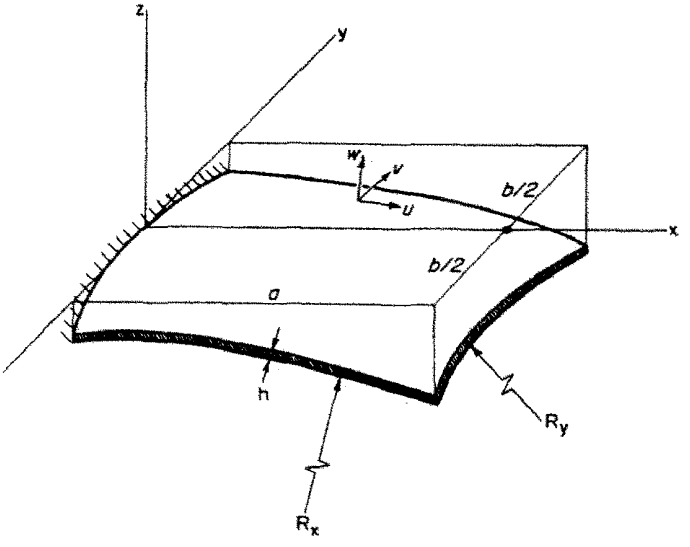

Fig. 2. Cantilevered doubly-curved shallow shell of rectangular planform.

expressed in terms of algebraic polynomials which exactly satisfy the clamped edge conditions. The accuracy of the method is established by convergence studies, and then the procedure is used to determine the effects of changing curvature, aspect, thickness and Poisson's ratios upon the vibration characteristics of cantilevered shallow shells.

2. ANALYSIS

Consider a doubly-curved, shallow shell having a midsurface determined by the surface

$$z(x, y) = \sum_{i,j} a_{ij} x^i y^j \tag{1}$$

(see Fig. 2), where the xy-plane is the reference base plane chosen so that it is tangent to the surface at the center of the clamped edge; i.e.

$$z(0,0) = \frac{\partial z}{\partial x}(0,0) = \frac{\partial z}{\partial y}(0,0) = 0. \tag{2}$$

Enforcing eqns (2) results in the constants of rigid body translation (a_{00}) and rotation (a_{10} and a_{11}) of the polynomial being eliminated. Assuming that the shell is shallow and, hence, that the squares and products of the local slopes $\partial z/\partial x$ and $\partial z/\partial y$ are small in comparison with unity,

$$\left(\frac{\partial z}{\partial x}\right)^2 \ll 1, \frac{\partial z}{\partial x}\frac{\partial z}{\partial y} \ll 1, \left(\frac{\partial z}{\partial y}\right)^2 \ll 1 \tag{3}$$

then the curvatures $1/R_x$ and $1/R_y$, and the twist $1/R_{xy}$, of the middle surface reduce to

$$\frac{1}{R_x} = -\frac{\partial^2 z}{\partial x^2}, \frac{1}{R_y} = -\frac{\partial^2 z}{\partial y^2}, \frac{1}{R_{xy}} = -\frac{\partial^2 z}{\partial x \partial y}. \tag{4}$$

Let us limit the analysis to shells having no twist ($1/R_{xy} = 0$) and constant curvature. The equation of the midsurface then becomes.

$$z = -\frac{1}{2}\left(\frac{x^2}{R_x} + \frac{y^2}{R_y}\right). \tag{5}$$

The strain energy of a shell undergoing stretching and bending is (*cf.* [11, 12])

$$V = V_m + V_b \tag{6}$$

where the stretching (or membrane) strain energy is given by

$$V_m = \frac{Eh}{2(1-\nu^2)} \int_{-b/2}^{b/2} \int_0^a \left\{(\epsilon_x + \epsilon_y)^2 - 2(1-\nu)\left(\epsilon_x \epsilon_y - \frac{\gamma_{xy}^2}{4}\right)\right\} dx\, dy \tag{7}$$

and the bending strain energy is

$$V_b = \frac{Eh^3}{12(1-\nu^2)} \int_{-b/2}^{b/2} \int_0^a \{(\kappa_x + \kappa_y)^2 - 2(1-\nu)(\kappa_x \kappa_y - \tau_{xy}^2)\}\, dx\, dy \tag{8}$$

where in the present analysis the integration is taken over the projected rectangular planform having dimensions $a \times b$ in the xy base plane (see Fig. 2).

For untwisted shallow shells the membrane strains are related to the tangential (u, v) and normal (w) displacements by (*cf.* [13])

$$\epsilon_x = \frac{\partial u}{\partial x} + \frac{w}{R_x}$$

$$\epsilon_y = \frac{\partial v}{\partial y} + \frac{w}{R_y} \tag{9}$$

$$\gamma_{xy} = \frac{\partial v}{\partial x} + \frac{\partial u}{\partial y}$$

and the curvature changes κ_x, κ_y, τ_{xy} are related to the displacements by

$$\kappa_x = \frac{\partial^2 w}{\partial x^2}, \kappa_y = \frac{\partial^2 w}{\partial y^2}, \tau_{xy} = \frac{\partial^2 w}{\partial x \partial y}. \tag{10}$$

The u and v displacement components (see Fig. 2) are in directions parallel to the xz- and yz-planes, respectively.

For shells undergoing free vibrations the displacements may be written as

$$u(x, y, t) = U(x, y) \sin \omega t$$

$$v(x, y, t) = V(x, y) \sin \omega t \tag{11}$$

$$w(x, y, t) = W(x, y) \sin \omega t$$

where ω is the circular frequency. Furthermore, if U, V and W are represented by the algebraic polynomials

$$U(x, y) = \sum_{i=1}^{I} \sum_{j=0}^{J} A_{ij} x^i y^j$$

$$V(x, y) = \sum_{k=1}^{K} \sum_{l=0}^{L} B_{kl} x^k y^l \tag{12}$$

$$W(x, y) = \sum_{m=2}^{M} \sum_{n=0}^{N} C_{mn} x^m y^n$$

then the geometric boundary conditions at the clamped edge, namely

$$U(0, y) = V(0, y) = W(0, y) = \frac{\partial W}{\partial x}(0, y) = 0. \tag{13}$$

are satisfied exactly and, as the upper limits $I, \ldots, N$ of the summations in eqns (12) are allowed to increase, mathematically complete sets of functions are generated which are capable of representing arbitrary displacements as closely as desired.

The coefficients A_{ij}, B_{kl}, C_{mn} will be determined by the Ritz method. That is, the functional $T_{max} - V_{max}$ is minimized, where V_{max} is the maximum total strain energy of deformation, occurring in the position of maximum displacement during vibration, and equal to the sum of eqns (7) and (8), with u, v and w replaced by U, V and W in eqns (9), and T_{max} is the maximum kinetic energy, occurring in the position of maximum velocity, and hence given by

$$T_{max} = \frac{\rho h \omega^2}{2} \int_{-b/2}^{b/2} \int_0^a (U^2 + V^2 + W^2)\, dx\, dy \tag{14}$$

with ρ the mass density per unit volume and h the shell thickness. The minimizing equations are

$$\frac{\partial (T_{max} - V_{max})}{\partial A_{ij}} = 0 \; (i = 1, \ldots, I; j = 0, \ldots, J) \tag{15a}$$

$$\frac{\partial (T_{max} - V_{max})}{\partial B_{kl}} = 0 \; (k = 1, \ldots, K; l = 0, \ldots, L) \tag{15b}$$

$$\frac{\partial (T_{max} - V_{max})}{\partial C_{mn}} = 0 \; (m = 2, \ldots, M; n = 0, \ldots, N) \tag{15c}$$

yielding a total of $I(J+1) + K(L+1) + (M-1)(N+1)$ simultaneous, linear, algebraic equations in the same number of unknowns A_{ij}, B_{kl}, C_{mn}. For a nontrivial solution the determinant of the coefficient matrix is set equal to zero. This yields $I(J+1) + K(L+1) + (M-1)(N+1)$ real eigenvalues, which are non-dimensional frequency parameters, and are upper bounds on the exact frequency parameters. The eigenvectors and, hence, eigenfunctions determining the free

vibration mode shapes are obtained by substituting the eigenvalues back into eqns (15), one at a time, in the usual manner.

For the present problem utilizing the coordinates shown in Fig. 2 to treat shells having double curvature, but no twist ($1/R_{xy} = 0$), the xz-coordinate axes establish a symmetry plane, and all vibration modes divide into two classes, which are either symmetric or antisymmetric with respect to the xz-plane. Recognition of the two symmetry classes permits one to separate the overall problem into two which are computationally smaller and more efficient. To do so, one chooses j, $n = 0, 2, \ldots$ and $l = 1, 3, \ldots$ in eqns (12) to obtain the symmetric modes; and j, $n = 1, 3, \ldots$ and $l = 0, 2, \ldots$ for the antisymmetric modes.

Further computational cost savings may be obtained by elimination of tangential inertia (*cf.*[5, 14]). This is accomplished by simply dropping the terms U^2 and V^2 in the kinetic energy functional (14), and algebraically eliminating the coefficients A_{ij} and B_{kl} from the minimizing eqns (15) before the eigenvalue determinants are evaluated. If equal numbers of terms in the polynomials for U, V and W are used, then the above elimination reduces the eigenvalue determinant to one-third of its previous size. However, the two-thirds which are eliminated are eigenvalues associated with modes which are predominantly U and/or V in character, and these modes are consequently missed entirely by the analysis. Furthermore, modes which are primarily flexural (W) are represented by frequencies which may be considerably too high, due to neglect of the tangential inertia. For the sake of more accurate numerical results, tangential inertia will be retained in the present work.

3. CONVERGENCE STUDIES

Convergence studies are made in order to obtain reasonable estimates of the accuracy of the numerical computations. In choosing the upper limits $I, \ldots, N$ of the summations in eqns (12) one must deal with the following considerations:

(a) Whether to assign equal or unequal numbers of degrees of freedom in each *direction* (i.e. x or y).

(b) Whether to assign equal or unequal numbers of degrees of freedom with each *displacement* (i.e. U, V or W).

Examples of the first type of convergence study are given by Tables 1 and 2. Here the changes in the frequency parameter $\omega a^2\sqrt{\rho h/D}$, where D is the usual flexural rigidity parameter

$$D \equiv \frac{Eh^3}{12(1-\nu^2)} \tag{16}$$

for shells of negative ($R_y/R_x = -1$) and positive ($R_y/R_x = 1$) Gaussian curvature having square planform ($a/b = 1$), moderate thickness ($b/h = 100$), and significant y-curvature ($b/Ry = 0.5$) are observed as the numbers of terms in the polynomial are increased in the x and y directions. In this case each displacement has equal degrees of freedom. Frequency parameters for the first four modes of each symmetry class are presented. As expected, they are all seen to converge monotonically from above.

The 4×2 solution in Tables 1 and 2 represents, for example, 4 terms of the polynomials (12)

Table 1. Directional convergence study of $\omega a^2\sqrt{\rho h/D}$ for $R_y/R_x = -1$ (hyperbolic paraboloidal), $a/b = 1$, $b/h = 100$, $b/R_y = 0.5$, $\nu = 0.3$

Polynomial terms in each direction (x times y)	Determinant size	Symmetric modes				Antisymmetric modes			
		1	2	3	4	1	2	3	4
4X2	24	9.7141	44.596	84.523	130.92	10.471	43.960	110.51	205.93
5X3	45	8.3455	37.209	73.753	103.72	9.4840	36.698	87.288	113.61
6X3	54	8.2787	36.962	73.008	101.34	9.4577	36.494	83.506	112.05
5X4	60	8.3132	36.742	73.184	101.70	9.4492	36.507	85.619	109.41
4X5	60	8.5890	37.918	78.173	106.54	9.5873	36.389	90.997	119.98
6X4	72	8.2429	36.503	72.331	99.151	9.4214	36.294	82.126	107.57
7X4	84	8.2360	36.463	72.154	98.917	9.4131	36.273	81.823	107.28
6X5	90	8.2364	36.485	72.289	99.090	9.4200	36.284	82.085	107.44

Table 2. Directional convergence study of $\omega a^2\sqrt{\rho h/D}$ for $R_y/R_x = 1$ (spherical), $a/b = 1$, $b/h = 100$, $b/R_y = 0.5$, $\nu = 0.3$

Polynomial terms in each direction (x times y)	Determinant size	Symmetric modes				Antisymmetric modes			
		1	2	3	4	1	2	3	4
4X2	24	10.100	37.298	66.980	130.40	10.279	41.586	109.20	220.02
5X3	45	9.1872	30.949	50.667	97.958	9.8392	34.512	77.348	105.56
6X3	54	9.0649	30.624	49.950	91.409	9.7931	34.223	73.891	101.80
5X4	60	9.1538	30.803	49.894	95.656	9.8269	34.283	75.306	100.59
4X5	60	9.8281	30.934	53.178	108.94	10.016	37.162	80.070	115.79
6X4	72	9.0327	30.476	49.237	89.361	9.7809	33.998	72.253	96.738
7X4	84	9.0154	30.427	49.083	88.657	9.7678	33.969	71.945	95.964
6X5	90	9.0272	30.467	49.201	89.156	9.7792	33.986	72.193	96.557

in the x-direction ($i = k = m - 1 = 1, 2, 3, 4$) and 2 terms in the y-direction ($j = n = 0, 2$ and $l = 1, 3$ for the symmetric modes; $j = n = 1, 3$ and $l = 0, 2$ for the antisymmetric modes). Each displacement therefore has 8 total terms in its polynomial and, hence, 8 degrees of freedom. The total number of degrees of freedom associated with all three displacements is therefore $3 \times 8 = 24$, which is the size of the frequency determinant.

Comparing 5×4 with 4×5 solutions in Tables 1 and 2, it is seen that the former is much better; that is, the frequencies are considerably lower, and therefore closer upper bounds on the exact values. This is one indication that more terms should be taken in the x- than the y-direction. However, if advantage were not taken of the symmetry, the 5×4 solutions would be 5×8 solutions, indicating that terms of higher algebraic *degree* are actually needed by the shell in the y-direction.

Tables 1 and 2 both show additional significant improvements in the frequencies as 5×4 is increased to 6×4, especially for a few of the higher frequency modes listed, but no significant further improvement in the first 8 modes is obtained by adding still another term in either direction (i.e. 6×5 or 7×4), so the 6×4 solution is considered reasonably well convergent. The substantial improvement of the 6×4 solution over the 6×3 and 5×4 solutions, and insignificant further improvement arising from larger solutions, is given quantitative documentation with Table 3. Inasmuch as computer time and cost increase approximately with the cube of the determinant size, the 6×4 solutions cost only about half as much as the 7×4 or 6×5, and are therefore more desirable. Similar results were found[5] for circular cylindrical shells ($R_y/R_x = 0$); in this case 5×4 solutions were sufficiently accurate.

Considering solution types of comparable determinant size for wider ($a/b = 0.5$) and narrower ($a/b = 2$) shells having all other geometric parameters the same, one finds that the 5×5 and 8×3 solutions, respectively, are optimum. If instead the thickness alone is increased ($b/h = 20$), the 5×4 solution is adequate; however, for thinner shells ($b/h = 500$), more terms in the x-direction (8×4) are needed.

Table 4 is a typical convergence study showing the effects of giving additional numbers of degrees of freedom selectively to each *displacement*. The geometric shell parameters used are the same as those of Tables 1 and 2. Beginning with a solution having $4 \times 2 = 8$ polynomial terms assigned equally to U, V and W, additional terms are added successively to each of the displacements, until each has $6 \times 4 = 24$ terms. For the example of Table 4 it is seen that giving

Table 3. Differences in first eight frequency parameters between 6×4 solutions and others (per cent)

Solution being compared with 6X4	$R_y/R_x = -1$		$R_y/R_x = 1$	
	Average difference	Maximum difference	Average difference	Maximum difference
6X3	1.42%	3.99%	1.56%	4.97%
5X4	1.48	4.15	2.44	6.63
7X4	-.18	-.37	-.36	-.80
6X5	-.06	-.12	-.09	-.25

Table 4. Displacement convergence study of $\omega a^2\sqrt{\rho h/D}$ for the shells of Tables 1 and 2

R_y/R_x	Polynomial terms in each direction U	V	W	Determinant size	Symmetric modes 1	2	3	4	Antisymmetric modes 1	2	3	4
-1	4X2	4X2	4X2	24	9.7141	44.596	84.523	130.92	10.471	43.960	110.51	205.93
	6X4	4X2	4X2	40	8.9676	40.328	77.725	113.34	10.312	40.063	106.01	204.74
	$\overline{4X2}$	6X4	4X2	40	9.6417	44.205	84.079	125.79	9.8959	41.200	95.074	138.38
	4X2	$\overline{4X2}$	6X4	40	9.1477	42.249	82.553	128.03	10.342	42.850	106.54	192.01
	6X4	6X4	$\overline{6X4}$	72	8.2429	36.503	72.331	99.151	9.4214	36.294	82.126	107.57
1	4X2	4X2	4X2	24	10.100	37.298	66.980	130.40	10.279	41.586	109.20	220.02
	6X4	4X2	4X2	40	9.4814	33.063	54.146	111.22	10.130	37.963	101.75	215.40
	$\overline{4X2}$	6X4	4X2	40	9.9305	36.630	66.510	112.60	10.072	38.477	85.230	132.45
	4X2	$\overline{4X2}$	6X4	40	9.5090	35.882	65.252	124.08	10.114	40.362	104.36	201.19
	6X4	6X4	$\overline{6X4}$	72	9.0327	30.476	49.237	89.361	9.7809	33.998	72.253	96.738

additional freedom to the axial (U) displacements is most important for five of the modes, whereas additional V displacement freedom is particularly desirable for the other three. The normal displacement (W) is least important. However, for thicker shells ($b/h = 20$), it is found that the W displacements are most important in obtaining accurate solutions.

Convergence studies have also been made for the case when $R_y/R_x = 0$ (i.e. cantilevered circular cylindrical shallow shells), including comparisons with convergence rates obtained from various finite element solutions[5, 14]. It was found that the present method required typically 1/3 to 1/2 as many degrees of freedom as finite element solutions for the same accuracy. Even considering the fact that the frequency determinants generated by finite element methods are banded and sparsely populated, and advantage may therefore be taken of specialized determinant evaluation techniques, the present method was found to be still more efficient.

4. RESULTS FOR SHELLS OF SQUARE PLANFORM

In the present section a study is made of the effects of changing the spanwise curvature ($1/R_x$) as the chordwise curvature ($1/R_y$) is held constant, thereby emphasizing the differences in frequencies and mode shapes from those of singly-curved ($1/R_x = 0$) shells. The comparison is made for shells having moderate geometric parameters (i.e. $a/b = 1$, $b/h = 100$) and a typical value of Poisson's ratio ($\nu = 0.3$). The effects of using more extreme values of these three parameters will be seen in Sections 5–7 which follow.

Figure 3 shows the change in the nondimensional frequency parameter $\omega a^2\sqrt{\rho h/D}$ for the first symmetric mode, which is predominantly spanwise (i.e. x-direction) bending, as the curvature ratio R_y/R_x is varied from -1 to 1. Four curves are drawn, beginning with that for a flat plate ($b/R_y = 0$) and changing the chordwise curvature ($1/R_y$). Thus, the change in circular frequency (ω) with changing $1/R_y$ is observed for fixed a, ρ, h, E and ν ($D = Eh^3/12(1-\nu^2)$) and fixed b(for $a/b = 1$) by changing b/R_y. As expected, increased chordwise curvature causes a considerable increase in the first spanwise bending frequency. However, giving the shell significant additional spanwise curvature, either positive or negative, is seen in Fig. 3 to cause an unexpected decrease in frequency. Figure 3 also shows that the maximum value of fundamental frequency occurs for shells having slightly positive Gaussian curvature, and that the points of maxima are shifted to the right with increasing b/R_y. More precise numerical results showing these trends is found in the first column of frequencies in Table 5, which are obtained using 6×4 solutions (i.e. eigenvalue determinants of order 72).

A previous study[7] devoted to the vibrations of doubly curved shells of rectangular planform supported on all sides by shear diaphragms showed that the fundamental vibration modes had frequencies considerably greater for shells of positive Gaussian curvature ($1/R_xR_y$) than those having negative values. Indeed, the hyperbolic paraboloid ($R_y/R_x = -1$) was found to have the same fundamental frequency as a flat plate, the circular cylinder ($R_y/R_x = 0$) a considerably larger value, and the sphere ($R_y/R_x = 1$) a still larger value. Figure 3 and Table 5 show the cylindrical curvature to be the stiffest (or nearly so—the exact frequency maxima are not exactly at $R_y/R_x = 0$) in the case of cantilevered edge conditions.

Table 5 also shows that the frequency of the first antisymmetric mode is increased due to

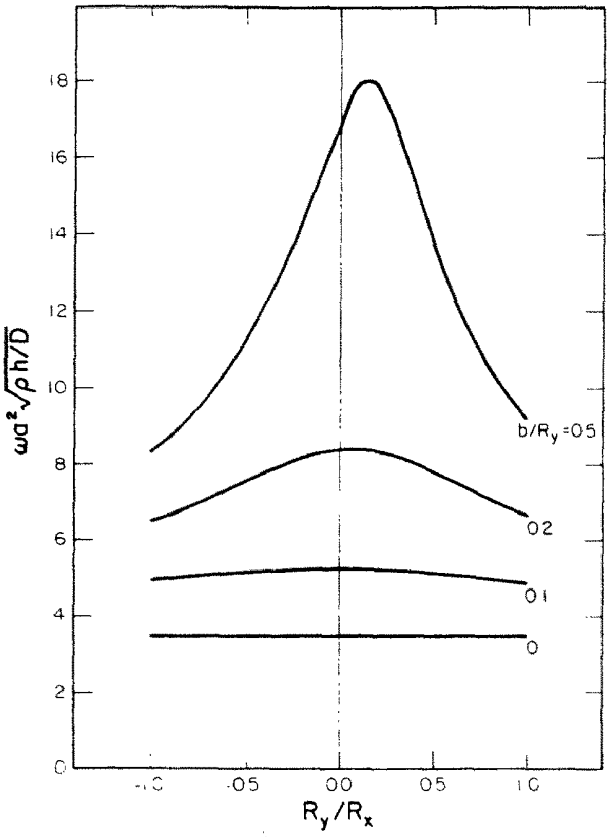

Fig. 3. First symmetric mode frequency as a function of curvature ratio ($a/b = 1$, $b/h = 100$, $\nu = 0.3$).

chordwise curvature, but additional spanwise curvature causes a slight reduction in frequency. This antisymmetric mode is predominantly torsional. The second antisymmetric mode frequencies behave in a similar manner, for this is also a torsional mode. The other modes, symmetric and antisymmetric, besides the three described above, yield frequencies which change in more complicated ways as R_y/R_x is changed. These higher frequency modes are more complicated, as will now be shown.

Figures 4(a) and (b) depict the first four mode shapes of each symmetry class by means of contours of normalized displacements W/W_{max}, for shells having significant chordwise cur-

Table 5. Nondimensional frequencies of doubly curved shells ($a/b = 1$, $b/h = 100$, $\nu = 0.3$)

$\frac{b}{R_y}$	$\frac{R_y}{R_x}$	$\omega a^2\sqrt{\rho h/D}$							
		Symmetric modes				Antisymmetric modes			
		1	2	3	4	1	2	3	4
0	All	3.4730	21.297	27.201	54.207	8.5114	30.973	64.164	71.023
0.1	-1.0	4.9440	25.795	32.758	56.767	8.5961	31.512	68.129	71.904
	-0.5	5.1414	26.358	28.589	54.968	8.6079	31.571	65.462	71.870
	0.0	5.2174	24.778	28.230	55.156	8.6138	31.565	64.325	72.042
	0.5	5.0840	23.229	30.140	57.249	8.6141	31.498	64.839	72.468
	1.0	4.8282	22.694	32.687	61.282	8.6090	31.385	66.366	73.486
0.2	-1.0	6.5038	29.931	46.125	65.010	8.8019	32.683	73.991	77.842
	-0.5	7.5071	30.165	38.974	57.203	8.8721	33.180	68.827	74.627
	0.0	8.3683	26.828	35.120	58.726	8.9063	33.249	64.646	75.030
	0.5	7.7655	24.664	36.566	67.387	8.8975	32.777	66.427	76.437
	1.0	6.5854	24.893	38.933	72.267	8.8553	32.161	68.789	80.677
0.5	-1.0	8.2429	36.503	72.331	99.151	9.4214	36.294	82.126	107.57
	-0.5	11.129	37.590	69.885	82.780	10.062	40.434	80.568	95.386
	0.0	16.991	30.650	47.704	90.217	10.595	42.234	65.585	90.029
	0.5	13.628	27.624	48.592	90.065	10.295	37.048	71.014	92.015
	1.0	9.0327	30.476	49.237	89.361	9.7809	33.998	72.253	96.738

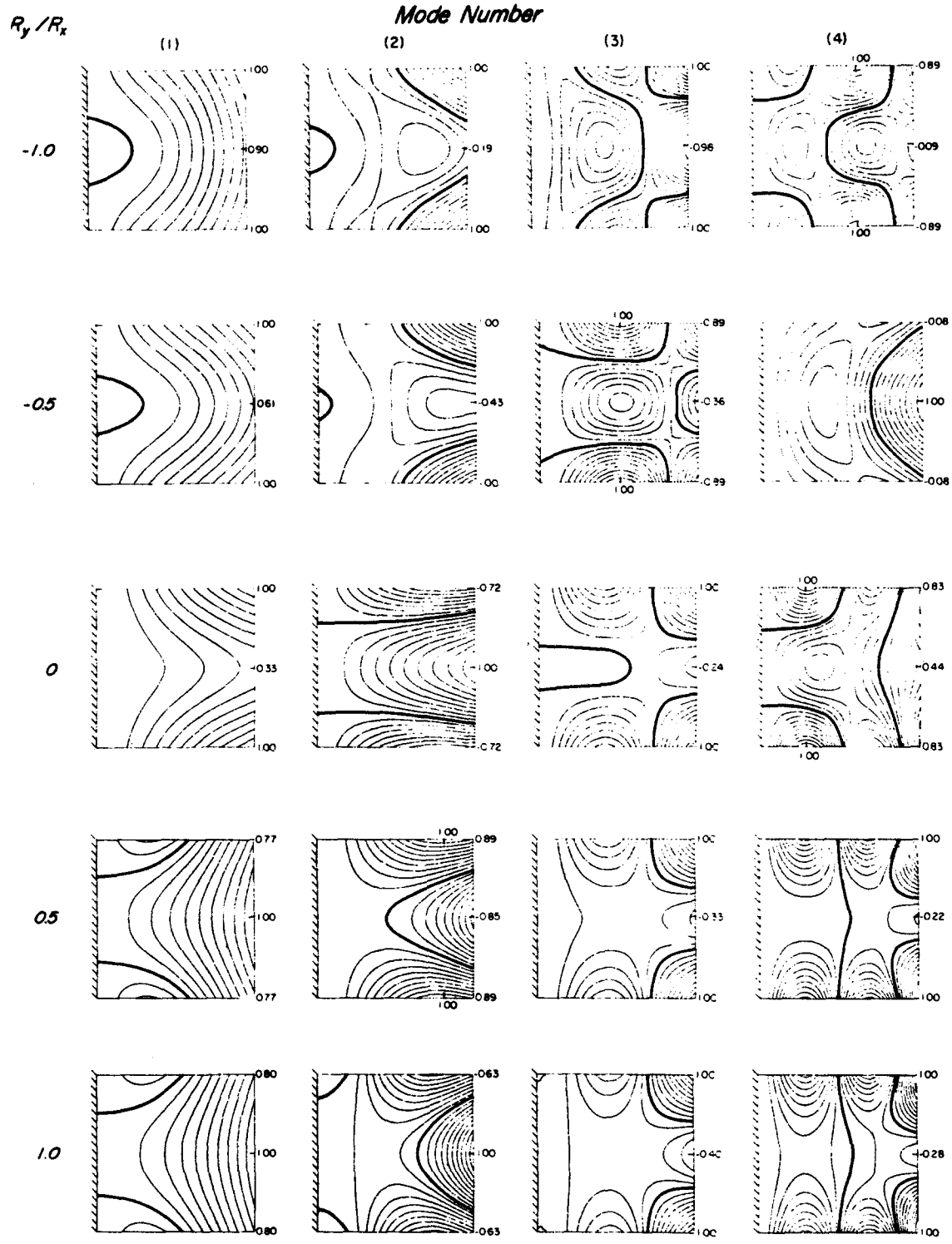

Fig. 4(a) Symmetric mode shapes for various R_y/R_x ($b/R_y = 0.5$, other data same as Table 5).

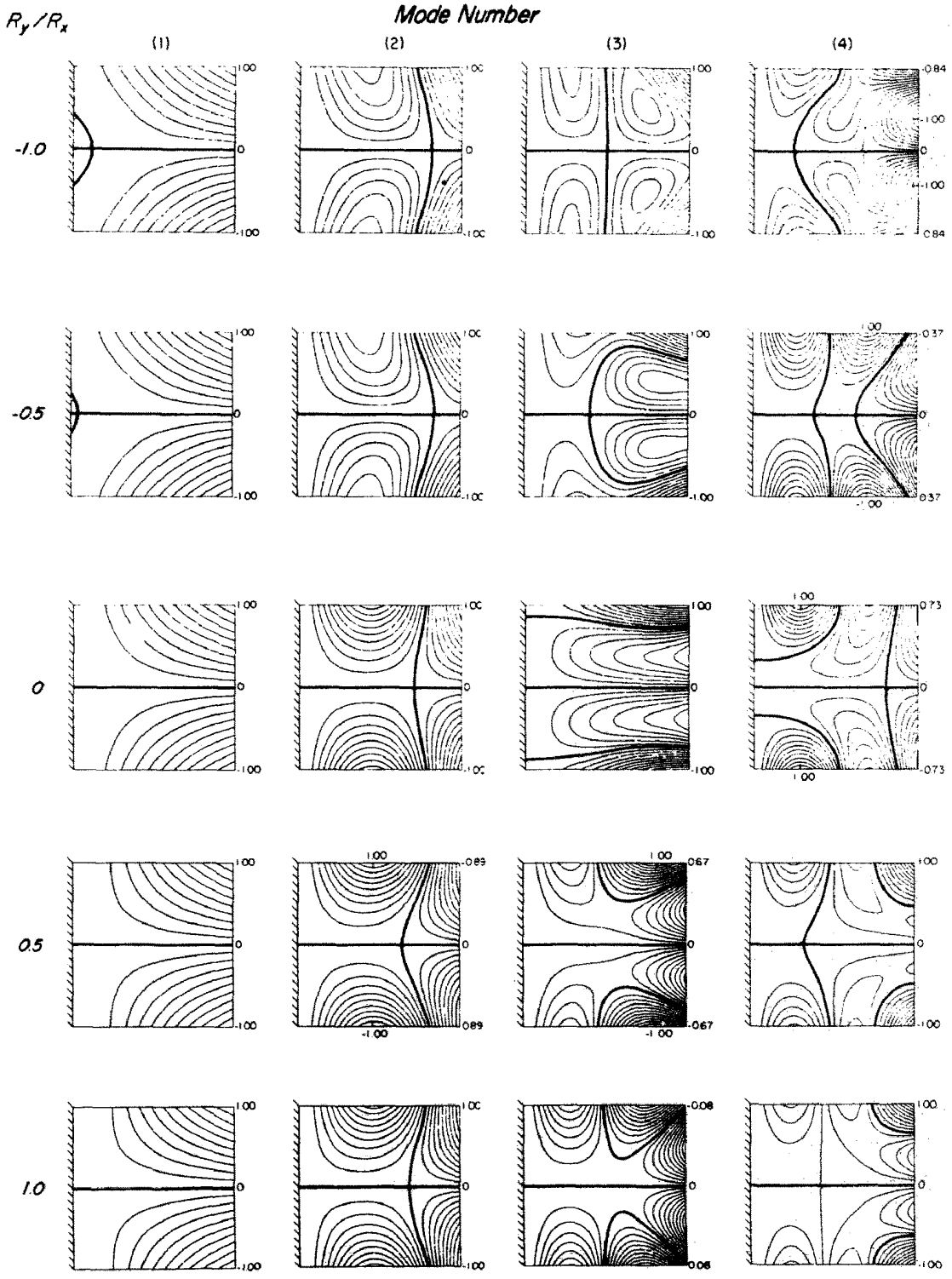

Fig. 4(b) Antisymmetric mode shapes for various R_y/R_x ($b/R_y = 0.5$, other data same as Table 5).

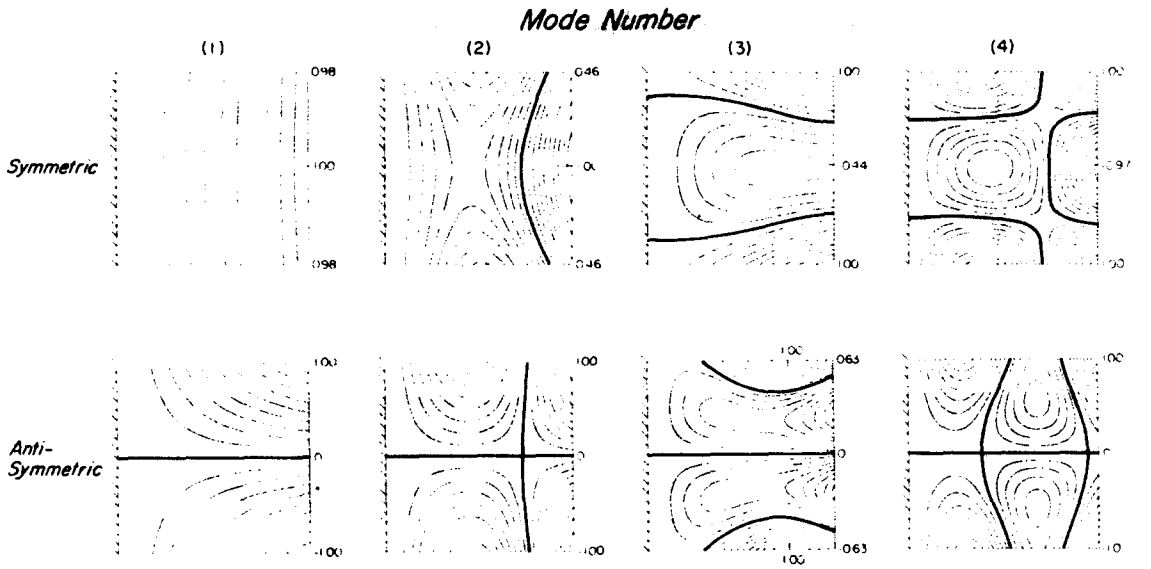

Fig. 5. Mode shapes of a flat square plate ($\nu = 0.3$).

vature ($b/R_y = 0.5$) and various degrees of spanwise curvature ($R_y/R_x = -1.0, -0.5, 0, 0.5, 1.0$). Zero displacement contour lines (i.e. node lines) are drawn more heavily in Figs. 4. The mode shapes correspond to the frequency parameters for $b/R_y = 0.5$ in Table 5. For comparison the contours of a flat plate ($b/R_y = 0$) are shown in Fig. 5.

The *first* symmetric mode of a flat plate shows contour lines which are nearly straight, lying in the y-direction (Figs. 2 and 5), indicating very little chordwise bending displacement. Figure 4(a) shows that the presence of chordwise curvature causes significant chordwise bending, and the contour lines are considerably curved. The slight anticlastic bending (i.e. less displacement in the corners than at the center) existing for the flat plate is seen in Fig. (4a) to be magnified for shells having positive R_y/R_x, but reversed for negative R_y/R_x. Considering the *second* symmetric modes, one observes that for $R_y/R_x = 1$ the mode resembles that of the flat plate (Fig. 4)—i.e. the second spanwise bending mode of the plate. However, as R_y/R_x approaches zero the second mode becomes similar to the third symmetric plate mode–i.e., chordwise bending. For negative R_y/R_x the second shell modes are predominantly corner bending. The third and fourth symmetric shell modes are more complicated superpositions of spanwise and chordwise bending.

Figure 4(b) depicts that the first antisymmetric mode is torsional, with the contour lines being nearly the same as those of the flat plate. Close comparison shows that the contour lines for positive R_y/R_x exhibit more severe curvature than those for the plate, whereas for negative R_y/R_x the lines are less curved, and for $R_y/R_x = 0$ the lines are virtually identical to those of the plate. The second antisymmetric mode in all cases is also similar to that of the plate (i.e. second torsional mode). The third and fourth modes differ considerably as R_y/R_x is changed. For only $R_y/R_x = 0$ does the antisymmetric chordwise bending mode (i.e. the third plate mode) exist in a relatively clear form. The presence of spanwise curvature in the other cases stiffens the shell considerably with respect to this mode, and causes strong coupling with torsion.

Consider now the shell having no chordwise curvature ($b/R_y = 0$). It would appear that the presence of spanwise curvature ($a/R \neq 0$) would have little effect upon the spanwise bending modes. This is verified by the first two columns of symmetric frequency parameters listed in Table 6. Similarly, the torsional modes are only slightly affected (first two columns of antisymmetric frequency parameters in Table 6). However, modes involving chordwise bending have their frequencies considerably changed by spanwise curvature. This is seen in the third symmetric mode of Table 6, which is predominantly chordwise bending.

5. EFFECTS OF ASPECT RATIO

Having seen the effects of curvature change upon the frequencies for shells of square planform ($a/b = 1$) in the previous section, let us now examine other aspect ratios, notably a wide shell ($a/b = 0.5$) and a narrow one ($a/b = 2.0$). Frequency parameters for cantilevered

Table 6. Nondimensional frequencies of singly-curved ($b/R_y = 0$) shells ($a/b = 1$, $b/h = 100$, $\nu = 0.3$)

$\frac{a}{R_x}$	$\omega a^2\sqrt{\rho h/D}$							
	Symmetric modes				Antisymmetric modes			
	1	2	3	4	1	2	3	4
0.0	3.4730	21.297	27.201	54.207	8.5114	30.973	64.164	71.023
0.2	3.4784	21.684	38.557	61.180	8.4788	30.734	69.036	77.632
0.5	3.4512	21.423	51.727	60.984	8.2942	29.554	68.383	98.001

Table 7. Frequency parameters $\omega a^2\sqrt{\rho h/D}$ for spherical shells ($R_y/R_x = 1$) for various aspect ratios and shallowness ratios ($b/h = 100$, $\nu = 0.3$)

$\frac{a}{b}$	$\frac{b}{R_x} = \frac{b}{R_y}$	Symmetric modes				Antisymmetric modes			
		1	2	3	4	1	2	3	4
0.5	0	3.4942	10.187	21.849	31.640	5.3540	19.085	24.683	43.118
	0.1	4.4816	10.254	22.573	32.042	5.4482	19.227	25.063	43.717
	0.2	6.4750	10.406	24.254	33.762	5.7050	19.545	26.100	45.575
	0.3	8.6069	10.572	26.007	35.785	6.0757	19.867	27.482	48.704
	0.5	10.852	12.454	28.898	39.138	6.9848	20.372	30.108	57.087
	1.0	11.494	18.082	35.953	45.276	9.2131	21.268	34.333	62.885
1	0	3.4730	21.297	27.201	54.207	8.5114	30.973	64.164	71.023
	0.1	4.8282	22.694	32.687	61.282	8.6090	31.385	66.366	73.486
	0.2	6.5854	24.893	38.933	72.267	8.8553	32.161	68.789	80.677
	0.3	7.7836	27.196	42.853	78.965	9.1671	32.889	70.239	89.835
	0.5	9.0327	30.476	49.237	89.361	9.7809	33.998	72.253	96.738
2	0	3.4435	21.452	60.206	93.166	14.810	48.205	92.590	160.14
	0.1	4.5317	25.875	68.332	116.43	14.742	47.526	93.158	154.86
	0.2	5.3997	30.581	77.383	127.78	14.497	45.548	93.826	158.51
	0.3	5.7810	33.448	84.353	135.57	14.060	43.635	94.020	162.08

Table 8. Frequency parameters $\omega a^2\sqrt{\rho h/D}$ for hyperbolic paraboloidal shells ($R_y/R_x = -1$) for various aspect ratios and shallowness ratios ($b/h = 100$, $\nu = 0.3$)

$\frac{a}{b}$	$\frac{b}{R_x} = -\frac{b}{R_y}$	Symmetric modes				Antisymmetric modes			
		1	2	3	4	1	2	3	4
0.5	0	3.4948	10.187	21.849	31.640	5.3540	19.085	24.683	43.118
	0.1	4.4271	10.895	22.660	31.731	5.4773	19.614	24.887	43.250
	0.2	5.7083	12.992	24.928	32.568	5.7782	21.057	25.537	43.679
	0.3	6.4819	15.902	28.160	34.016	6.1414	22.926	26.810	44.402
	0.5	7.2625	21.542	34.622	39.730	6.8157	25.843	31.929	46.778
	1.0	8.1023	38.324	49.819	52.494	7.8548	29.800	48.292	57.791
1	0	3.4730	21.297	27.201	54.207	8.5114	30.973	64.164	71.023
	0.1	4.9440	25.795	32.758	56.767	8.5961	31.512	68.129	71.904
	0.2	6.5038	29.931	46.125	65.010	8.8019	32.683	73.991	77.842
	0.3	7.4128	33.094	57.032	78.023	9.0423	33.983	76.732	88.608
	0.5	8.2429	36.503	72.331	99.151	9.4214	36.294	82.126	107.57
2	0	3.4435	21.452	60.206	93.166	14.810	48.205	92.590	160.14
	0.1	4.9593	29.428	76.864	127.17	14.699	47.423	92.999	155.15
	0.2	6.0005	36.645	95.145	152.75	14.357	45.435	93.886	160.40
	0.3	6.4026	40.502	106.71	169.82	13.797	43.100	94.914	167.16

spherical shells ($R_y/R_x = 1$) having these aspect ratios may be seen in Table 7 for a shell having moderate thickness ($b/h = 100$) and $\nu = 0.3$. Similar results for cantilevered hyperbolic paraboloidal shells ($R_y/R_x = -1$) are presented in Table 8. In both Tables 7 and 8 the limits of chordwise shallowness ratio b/R_y used are reduced with increasing a/b in order that the problems solved have sufficiently small spanwise shallowness ratio (a/R_x) to stay within acceptable bounds for shallow shell theory.

Convergence studies similar to those described in Section 3 were conducted to determine good solution sizes for the aspect ratios used in Tables 7 and 8. For results arising from

eigenvalue determinants of comparable size, 5×5, 6×4 and 8×3 solutions were found to be best suited for aspect ratios 0.5, 1 and 2, respectively.

6. EFFECTS OF THICKNESS RATIO

Results given previously have all been for a moderate thickness ratio ($b/h = 100$). To consider the differences arising for relatively thick ($b/h = 20$) and relatively thin ($b/h = 500$) shells, a small set of additional frequencies is presented in Table 9 for shells having square planform. To observe the changes in the actual frequencies as the thickness is changed, a thickness-independent frequency parameter $\omega a\sqrt{\rho/E}$ is used for Table 9; that is, this parameter, unlike the previously used $\omega a^2\sqrt{\rho h/D}$ does not contain h (one must remember that D is also a function of h).

In making convergence studies for the relatively thin shells ($b/h = 500$), it was found that additional terms were required in the displacement polynomials to obtain comparable convergence. Thus the results for $b/h = 20$, 100 and 500 were obtained using 7×4, 7×4 and 8×5 solutions, respectively.

Table 9 shows clearly that as the thickness is decreased (increasing b/h with fixed $b = a$), the frequencies all decrease, as would be expected. However, they do not decrease as for a flat plate, where the frequencies are proportional to the thickness. This is because of the membrane (stretching) effects in the shells, which become relatively more important as b/h increases. One observes that the spanwise bending frequencies (e.g. symmetric mode 1) are less strongly affected than the torsional frequencies (e.g. antisymmetric mode 1) by thickness changes, again indicating the relative importance of membrane effects in the former modes. It is also interesting to note that for very thin shells ($b/h = 500$) having the present edge conditions the torsional and first spanwise bending frequencies are almost the same (i.e., $0.6326 \sim 0.6677$ and $0.7881 \sim 0.7701$).

7. EFFECTS OF POISSONS RATIO

Table 10 shows the effects of changing Poisson's ratio upon the vibration frequencies of doubly curved cantilevered shells having representative aspect, thickness and chordwise curvature ratios of 1, 100 and 0.5, respectively. The nondimensional frequency parameter

Table 9. Thickness-independent frequency parameters $\omega a\sqrt{\rho/E}\times10^2$ for doubly-curved shells having various thickness ratios ($a/b = 1$, $b/R_y = 0.5$, $\nu = 0.3$)

R_y/R_x	b/h	Symmetric modes				Antisymmetric modes			
		1	2	3	4	1	2	3	4
-1	20	7.3199	37.990	49.294	85.314	12.581	44.315	70.458	103.27
	100	2.4923	11.034	21.835	29.934	2.8385	10.977	24.761	32.464
	500	.6326	2.6635	6.4003	11.354	.6677	3.0541	6.6835	11.438
1	20	7.1471	33.437	48.874	92.498	12.691	43.558	70.306	100.64
	100	2.7282	9.2076	14.853	26.829	2.9559	10.279	21.635	29.040
	500	.7881	2.2300	4.3390	8.3521	.7701	2.8884	5.5056	7.7923

Table 10. Effect of Poisson's ratio (ν) upon $\omega a\sqrt{\rho/E}\times10^2$ for $a/b = 1$, $b/R_y = 0.5$, $b/h = 100$

R_y/R_x	ν	Symmetric modes				Antisymmetric modes			
		1	2	3	4	1	2	3	4
-1	0	2.3311	10.817	22.546	30.346	3.0415	11.058	24.088	32.695
	0.3	2.4944	11.046	21.888	30.004	2.8510	10.983	24.852	32.552
	0.5	2.7347	11.661	22.028	30.465	2.8195	11.376	26.360	33.050
0	0	5.1927	9.4348	15.106	27.740	3.4225	13.327	19.439	27.820
	0.3	5.1417	9.2751	14.436	27.301	3.2062	12.781	19.847	27.244
	0.5	5.2130	9.4880	14.318	27.462	3.1390	12.643	20.935	27.560
1	0	2.9257	9.9916	15.940	28.288	3.2332	11.047	23.187	30.458
	0.3	2.7334	9.2225	14.900	27.042	2.9598	10.288	21.865	29.274
	0.5	2.6712	8.8807	14.474	26.770	2.8468	10.030	21.451	29.026

$\omega a\sqrt{\rho/E}$, which does not contain ν, is again tabulated, permitting one to observe directly the change in ω due to changing ν. Results in Table 10 were obtained from 6×4 solutions.

The following conclusions regarding the first eight modes are apparent from Table 10:

(a) For spherical shells ($R_y/R_x = 1$) the frequencies of all modes decrease with increasing ν.

(b) For circular cylindrical and hyperbolic-paraboloidal shells ($R_y/R_x = 0, -1$) no distinct trend is observed; with increasing ν, frequencies increase, decrease or vary nonmonotonically, depending upon the particular mode in question.

These variations in the latter cases may be explained by the fact that increased elastic coupling due to increased ν affects the inertia of the system, as well as the stiffness, the relative importance of each being determined by the geometric parameters of the problem and by the type of deformation exhibited by a particular mode shape.

8. CONCLUSIONS

The Ritz method using displacement functions in the form of algebraic polynomials is a good procedure for solving free vibration problems for cantilevered doubly-curved shallow shells of rectangular planform. Accurate results may be obtained with a reasonable number of terms.

The addition of spanwise curvature to cantilevered shells already having chordwise curvature is seen to decrease the frequencies of the spanwise bending and torsional modes, which are typically the lowest frequencies. Unlike the classical case of a shell supported on all sides by shear diaphragms, for which an exact, closed form solution exists, it is seen in the present problem that shells having negative Gaussian curvature (i.e. R_y/R_x negative) will have frequencies in some modes greater than those having the same magnitude of positive Gaussian curvature.

Studies made with independent variation of aspect ratio, thickness ratio and Poisson's ratio show no clearly definable general trends. Each mode must be looked at separately to observe frequency changes resulting from changing geometric parameters. The numerical results presented for this previously unsolved problem should be useful to designers and researchers in the future for estimating the effects of double curvature upon shell vibrations.

Acknowledgement—This work was carried out with the support of the National Aeronautics and Space Administration, Lewis Research Center, under Grant No. NAG 3-36.

REFERENCES

1. A. W. Leissa, *Vibration of Shells*. U.S. Govt. Printing Office, Washington, D. C. (1973).
2. M. D. Olson and G. M. Lindberg, Vibration analysis of cantilevered curved plates using a new cylindrical shell finite element. *Proc. 2nd Conf. Matrix Meth. Struct. Mech.*, AFFDL-TR-68-150, p. 200 (1969).
3. M. D. Olson and G. M. Lindberg, Dynamic analysis of shallow shells with a doubly-curved triangular element. *J. Sound Vib.* **19**, 283 (1971).
4. K. P. Walker, Vibrations of cambered helicoidal fan blades. *J. Sound Vib.* **59**, 35 (1978).
5. A. W. Leissa, J. K. Lee and A. J. Wang, Vibrations of cantilevered shallow cylindrical shells having rectangular planform. *J. Sound Vib.* **78**, 311 (1981).
6. A. W. Leissa, Vibrations of turbine engine blades by shell analysis. *Shock Vib. Digest* **12**, 3 (1980).
7. A. W. Leissa and A. S. Kadi, Curvature effects on shallow shell vibrations. *J. Sound Vib.* **16**, 173–187 (1971).
8. K. Marguerre, Zur Theorie der gekrümmten Platte grosser Formänderung. *Proc. 5th Int. Cong. Appl. Mech.*, 93 (1938).
9. E. *Reissner, Stresses and displacements of shallow spherical shells. J. Math. Phys.* **25**, 80 (1946); **26**, 279 (1947).
10. V. Z. Vlasov, *General Theory of Shells and its Applications in Engineering* (English translation). NASA TTF-99 (1964).
11. A. L. Goldenveizer, *Theory of Thin Shells*. Pergamon Press, New York (1961).
12. V. V. Novozhilov, *The Theory of Thin Elastic Shells*. Noordhoff, Groningen (1964).
13. F. W. Niedenfuhr, A. W. Leissa and M. J. Gaitens, A method of analysis for shallow shells of revolution supported elastically on concentric rings. *Devel. Theor. Appl. Mech.* **2**, 47 (1965).
14. A. W. Leissa, J. K. Lee and A. J. Wang, Rotating blade vibration analysis using shells, ASME Paper No. 81-GT-80. *J. Engng Power* to appear.